

Effects of End-Block Associating Homopolymers on the Thermomechanical Properties and Phase Behavior of a Triblock Copolymer

J. P. Baetzold[†] and J. T. Koberstein*

Department of Chemical Engineering and Polymer Program, Institute of Materials Science, University of Connecticut, Storrs, Connecticut 06269-3136

Received May 26, 2000

ABSTRACT: The effects of low molecular weight poly(xylenyl ether) (PXE) homopolymers on the phase behavior and thermomechanical properties of a poly{styrene-*b*-(ethylene-*co*-butylene)-*b*-styrene} triblock copolymer (SEBS) are reported. The PXE homopolymers associate with the polystyrene (PS) end blocks of the copolymer and lead to significant property enhancements, including elevation and extension of the rubbery plateau, an increase in the room temperature shear modulus, elevation of the glass transition of the glassy microphase, and an increase in the order–disorder transition temperature. The broad nature of the loss transitions for the mixed microphase of PS and PXE indicates that solubilized PXE is heterogeneously distributed within the PS microdomains, locating preferentially at the center of the microdomain. Miscibility of the homopolymers within the end-block microdomains is limited as evidenced by the observation of macrophase formation above a critical homopolymer concentration. Experimental phase and property information is used to construct a phase diagram for the blend system. At low temperatures, the phase diagram is dominated by upper critical solution temperature behavior associated with the repulsive interactions of PXE with the EB midblock. At high temperatures, the phase diagram exhibits lower critical solution temperature behavior consistent with the known phase behavior of blends of PXE with polystyrene homopolymers.

Introduction

It has become common practice to use various homopolymers to modify the properties of block copolymers. In the case of styrene–diene–styrene ABA type triblock copolymers, typical polymeric modifiers include polystyrene to increase the modulus¹ and tackifiers² to improve adhesive properties. Because of their commercial importance, the phase behavior of A/ABA or B/ABA block copolymer blends with one of the corresponding homopolymers has been studied in some detail. Roe³ and Han,⁴ for example, have presented phase diagrams that map out regions of optimal use, processing regions, and solubility limits.

Several investigators have also investigated block copolymer blends where the homopolymer is unlike either block copolymer sequence. Paul et al.⁵ studied blends of poly(xylenyl ether) (PXE) with poly(styrene-*b*-butadiene-*b*-styrene) (SBS) and poly{styrene-*b*-(ethylene-*co*-butylene)-*b*-styrene} triblock copolymers and found that the solubility of PXE in the poly(styrene) (PS) microphase was much greater than that of PS homopolymer because of the greater exothermic heat of mixing. Glass transition temperature analysis indicated that the homopolymers were dissolved within the block copolymer microdomains even when the molecular weight ratio of the homopolymer to the styrene block was greater than unity. Thermal analysis, however, is often incapable of detecting phase separation at small extents. Some macrophase separation was evidenced by

the fact that transmission electron microscopy detected large dark regions, consistent with the existence of macrophases, in blends that displayed a single glass transition temperature.⁶ Hashimoto reported similar behavior⁷ in studies of the effects of PXE homopolymer on the phase behavior of a poly(styrene-*b*-isoprene) diblock copolymer. The morphology depended strongly on the sample preparation method and relative ratio of homopolymer to styrene block molecular weight.

This paper examines the phase behavior of a poly{styrene-*b*-(ethylene-*co*-butylene)-*b*-styrene} triblock copolymer (SEBS) blended with poly(xylenyl ether) homopolymers of varying molecular weight. The effects of these added homopolymers on morphological behavior are reported elsewhere.⁸

Experimental Section

Materials. A poly{styrene-*b*-(ethylene-*co*-butylene)-*b*-styrene} triblock copolymer (SEBS-1) was chosen as the base material. The material is based on a poly(styrene-*b*-butadiene-*b*-styrene) precursor that was prepared by sequential polymerization and was subsequently hydrogenated and characterized at the Shell Development Co. From proton NMR measurements before hydrogenation, the midblock microstructure was determined to be 37.5% 1,2-butadiene and the weight percent of PS was estimated to be 28.1.⁹ Gel permeation chromatography (GPC) analysis on the hydrogenated material gave a number-average molecular weight of 30 800 g/mol and a polydispersity of 1.09. The GPC data were corrected for differences in hydrodynamic volumes between the PS and the hydrogenated poly(butadiene) or ethylene-*co*-butylene (EB) materials, leading to number-average molecular weights of 3400 g/mol for each PS end block and 14 600 g/mol for the EB midblock. The corresponding weight percent of PS in the block copolymer is 31.8%.

Three samples of poly(2,6-dimethyl 1,4-phenylene oxide), also known as poly(xylenyl ether) (PXE), were provided by Dr. Roger Kambour of the General Electric Co. A step polymeri-

[†] Current address: 3M Display Technology Center, St. Paul, MN 55144-1000.

* To whom correspondence should be addressed. Current address: Department of Chemical Engineering, Columbia University, 500 W. 120th Street, New York, NY 10027. Telephone (212) 854-3120; FAX (212) 854-3054; e-mail jk1191@columbia.edu.

Table 1. Characteristics of PXE Homopolymers

| material designation | M_n from GPC | M_w/M_n from GPC | M_n from VPO | T_g (°C) from DSC |
|----------------------|----------------|--------------------|----------------|---------------------|
| PXE-1 | 1593 | 2.29 | 1032 | 116 |
| PXE-2 | 2678 | 1.7 | 1857 | 161 |
| PXE-6 | 6043 | 1.93 | 5751 | 196 |

zation involving oxidative coupling¹⁰ was used in preparing the materials. The properties of the PXE materials are summarized in Table 1. The number in the sample designation indicates the nominal number-average molecular weight in thousands. GPC was used to determine the styrene equivalent molecular weights and polydispersities. Absolute number-average molecular weights were determined with vapor phase osmometry. These values are lower than the PS equivalent values from GPC analysis.

Methods. Molecular weights (i.e., PS equivalent) and polydispersities were determined using a Waters automated GPC using a refractive index detector calibrated with PS standards. Tetrahydrofuran at a flow rate of 1.0 mL/min was employed as the mobile phase for sample concentrations of 5–10 mg/mL.

Vapor phase osmometry (VPO) calibration was performed using five benzil solutions ranging from 1.67 to 13.4 g/L in HPLC-grade toluene. The VPO was maintained at 40 °C, and three samples of each concentration were tested to find the average voltage reading. Each test sample was allowed to equilibrate for 3 min before a voltage reading was made. PXE solutions in the range 0.8 and 12 g/L were tested in a similar fashion.

Glass transition temperatures of the materials were determined with a Perkin-Elmer DSC-7 on samples weighing 8–20 mg. The materials were heated from 40 to 250 °C at 20 °C/min, and the glass transition temperatures were determined from the first temperature scan. The temperature was calibrated with an indium reference standard.

The occurrence of phase separation upon both heating and cooling in blends of PXE with SEBS renders sample preparation difficult. Many of the property changes induced by changes in temperature are irreversible because of this complex phase behavior. Solvent casting was selected to prepared thin film specimens because it provided the most consistent and reproducible means of sample preparation. While the reproducibility of experimental results was excellent, the possibility of non-equilibrium effects often observed when solvent casting is employed cannot be ruled out.

Thin films of the neat block copolymer and blends were prepared by casting 2 wt % solutions in toluene at room temperature in 1 in. diameter Teflon dishes. Solvent evaporation was controlled by placing an inverted mortar over the dishes and was complete after 7 days. The thickness was controlled by the amount of polymer used to make the solution and was approximately 0.6 mm. To remove solvent without causing bubble formation in the films, a two-step drying process was used. Samples were dried at 40 °C for 1 day under minimal vacuum and then for 3 days under vacuum at 70 °C. Constant weight was achieved after 3 days, indicating that most of the solvent had been removed. Since lower critical solution temperature behavior was expected for blends with PXE, specimens were annealed at 75 °C, slightly above the glass transition temperature of the PS microphase in the block copolymer.

A Polymer Laboratories dynamic mechanical thermal analyzer (DMTA) was used to characterize the mechanical properties of the materials studied. The bending head was configured with the shear sandwich test fixture. Two samples (7 mm in diameter and 0.6 mm thick) were mounted at room temperature under an applied force of 20 oz-in. placed against the sample bar. The peak-to-peak displacement was 32 μ m, and frequencies of 0.1, 0.2, 1, 5, and 10 Hz were chosen for the experiments. The system was programmed in temperature jump mode to collect modulus data from 50 to 300 °C at 2 °C intervals. Each sample was equilibrated for 2 min at each temperature before data acquisition, and a constant purge of

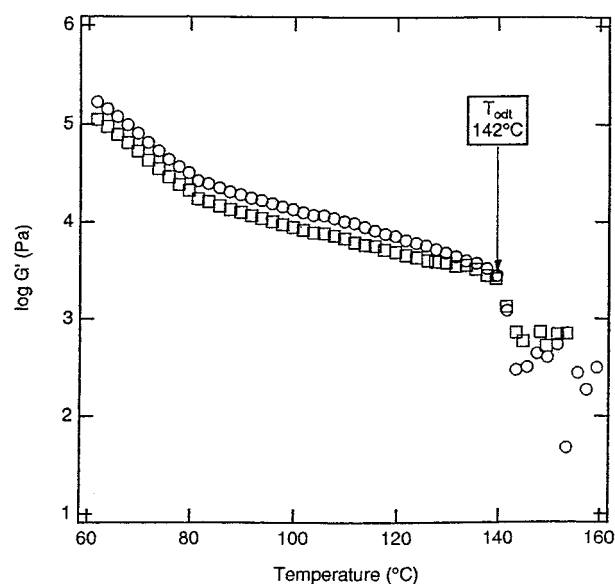


Figure 1. Temperature dependence of the dynamic shear storage modulus for two samples of neat SEBS-1 at a frequency of 0.1 Hz illustrating experimental reproducibility.

nitrogen was used to minimize sample degradation. The shear storage and loss modulus were determined for at least two samples from the same blend or neat SEBS-1 to determine the precision of measurements.

A Nikon PFX microscope and a Mettler FP52 hot stage with Mettler FP5 temperature controlling device were used to observe film flow behavior. Samples of 0.5 mm nominal thickness were placed between two coverslips and heated at 2 °C/min from 100 °C until flow was observed. The flow point was determined as the temperature at which the sample spread to about 0.1 mm in thickness when observed edge on. The top coverslip was required to force flow. Otherwise, the surface tension of the material upon reaching the flow temperature made it difficult to discern a change in state. Temperature calibration of the Mettler hot stage was conducted using the melting standards adipic acid ($T_m = 151.46 \pm 0.05$ °C) and chloroanthraquinone ($T_m = 208.95 \pm 0.05$ °C) provided by Mettler.

Results and Discussion

A. Dynamic Mechanical Properties. 1. Neat SEBS-1. The repeatability of the experimental dynamic mechanical measurements and sample preparation procedures is illustrated in Figure 1 where the temperature dependence of the shear storage modulus of the neat block copolymer is compared for two SEBS-1 samples prepared independently. The discontinuous drop observed in the shear modulus indicates the order–disorder transition temperature (T_{odt}).¹¹ Above this temperature, the data is noisy because of the difficulty in measuring the low modulus for the material in the disordered state.

The order–disorder transition temperatures are reproducible to within two degrees (141.6 and 143.6 °C) for the two samples. The T_{odt} for vacuum compression molded samples was found to be 142 °C, providing some evidence that the solvent evaporation method produces equilibrated samples. The loss tangent ($\tan \delta$) data shown in Figure 2 show that the single peak at 74 °C corresponding to the glass transition temperature of the PS microphase is also reproducible. A sharp increase in the $\tan \delta$ reveals the significant increase in molecular mobility that occurs above T_{odt} . At least two runs were performed for all the blends, and average transition

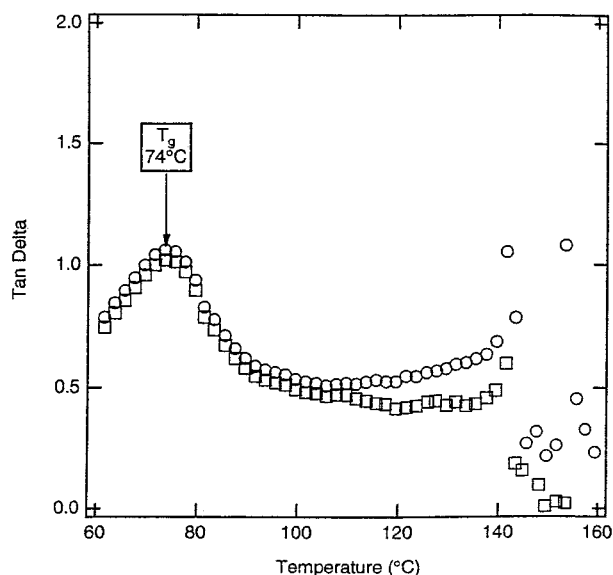


Figure 2. Tan δ as a function of temperature for two samples of neat SEBS-1 at a frequency of 0.1 Hz illustrating experimental reproducibility.

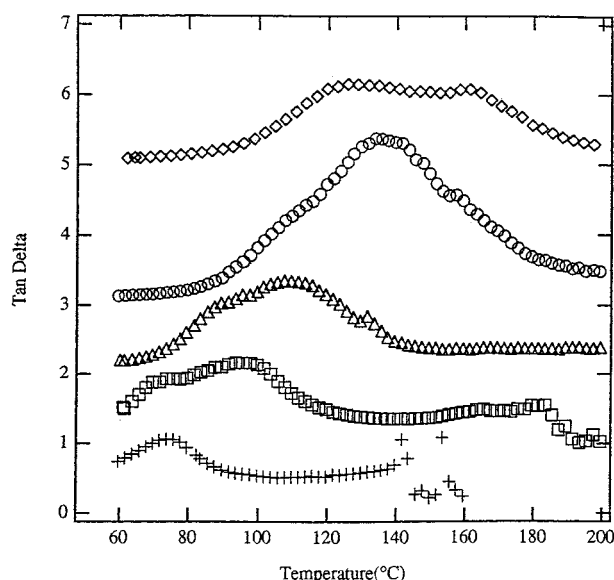


Figure 3. Tan δ as a function of temperature for blends of PXE-2 with SEBS-1. From bottom to top, the compositions are 0, 5, 10, 20, and 30 wt % PXE-2. The 5, 10, 20, and 30 wt % blend data are successively offset vertically by a factor of 1.0 to improve readability.

values are reported. Precision in the mechanical properties determined for the blends are similar to that shown for the two SEBS-1 samples in Figures 1 and 2. Quantitative analysis of the error in transition temperatures is difficult due to the broad nature of the transitions and the use of temperature-jump mode. Transition temperatures measured from multiple runs, however, are typically reproducible to within the temperature-jump interval of 2 °C.

2. Blends of PXE with SEBS-1: Concentration Effects. The dependence of tan δ on temperature for mixtures of 0–30% PXE-2 with SEBS-1 is shown in Figure 3 for data acquired at 0.1 Hz. These data illustrate qualitatively the interesting phase and microphase behavior of the blends. The neat block copolymer has a sharp unimodal loss peak at 74 °C associated with the glass transition temperature (T_g) of the PS micro-

phase of the block copolymer. The transition in tan δ near 150 °C is indicative of catastrophic loss resulting from flow of the disordered phase.

The tan δ data for the blends exhibit multimodal character. For example, the 5% blend (open squares in Figure 3) shows bimodal behavior with a primary loss visible as a maximum at 90 °C and a secondary loss appearing as a shoulder near 70 °C, the glass transition of the styrene block in neat SEBS-1. Qualitatively similar behavior is seen in the 10% blend, but the temperatures of both the primary and secondary loss transitions are elevated slightly. The lack of any loss transitions for the 5 and 10% blends near the expected glass transition of pure PXE-2 (Table 1) indicates that all of the PXE-2 in these blends is solubilized within the PS microdomains [Note: PXE-2 is not miscible with the poly(ethylene-*co*-butylene) block.] The broad nature of the loss transitions associated with solubilized PXE-2 suggests that the PXE homopolymer is heterogeneously distributed within the PS microdomains, consistent with the conclusions of an earlier study of blends of PXE with styrenic block copolymers.⁵

There are two obvious possibilities that can account for the heterogeneity in PXE-2 distribution for the 5% and 10% blends: either the heterogeneity is macroscopic, that is, the concentration of PXE is locally homogeneous within a single microdomain, but varies from microdomain to microdomain due to nonequilibrium effects associated with solvent casting,⁷ or the distribution is globally homogeneous, but there is a gradient of PXE concentration within each polystyrene microdomain. There currently is no theory available that treats the distribution of PXE within a SEBS triblock copolymer; however, theory¹² and experiment¹³ for A/A–B blends have confirmed the localization of type A homopolymers at the center of the A microdomains in A–B diblock copolymers, and electron microscopy analysis for the 5% and 10% PXE-2 blends does not reveal any large-scale heterogeneities. It is therefore reasonable to attribute the heterogeneity in PXE spatial distribution to a composition gradient across the PS microdomain.

Some insight into the nature of the PXE concentration gradient for these blends can be gained by estimating the glass transition temperatures for hypothetical blends wherein all of the PXE is homogeneously distributed within the polystyrene microdomains. These “mixed microphase” T_g 's are estimated by applying the Fox equation¹⁴ employed previously by Tucker et al.¹⁷ for blends of PXE with SBS copolymer. The Fox equation is

$$\frac{1}{T_g} = \frac{w_{\text{PXE}}}{T_{g,\text{PXE}}} + \frac{1 - w_{\text{PXE}}}{T_{g,\text{PS}}} \quad (1)$$

Here T_g is the glass transition temperature (in kelvin) of the mixture, w_{PXE} is the weight fraction of PXE, $T_{g,\text{PXE}}$ is the glass transition temperature of pure PXE, and $T_{g,\text{PS}}$ is the glass transition temperature of PS in neat SEBS.

The mixed microphase T_g 's predicted by the Fox equation (see Table 2) generally fall between the experimentally measured primary and secondary loss transition temperatures, supporting the existence of a gradient of solubilized PXE exhibiting regions of both depletion and of excess. Depletion of PXE is most likely to occur at the block copolymer interface because PXE

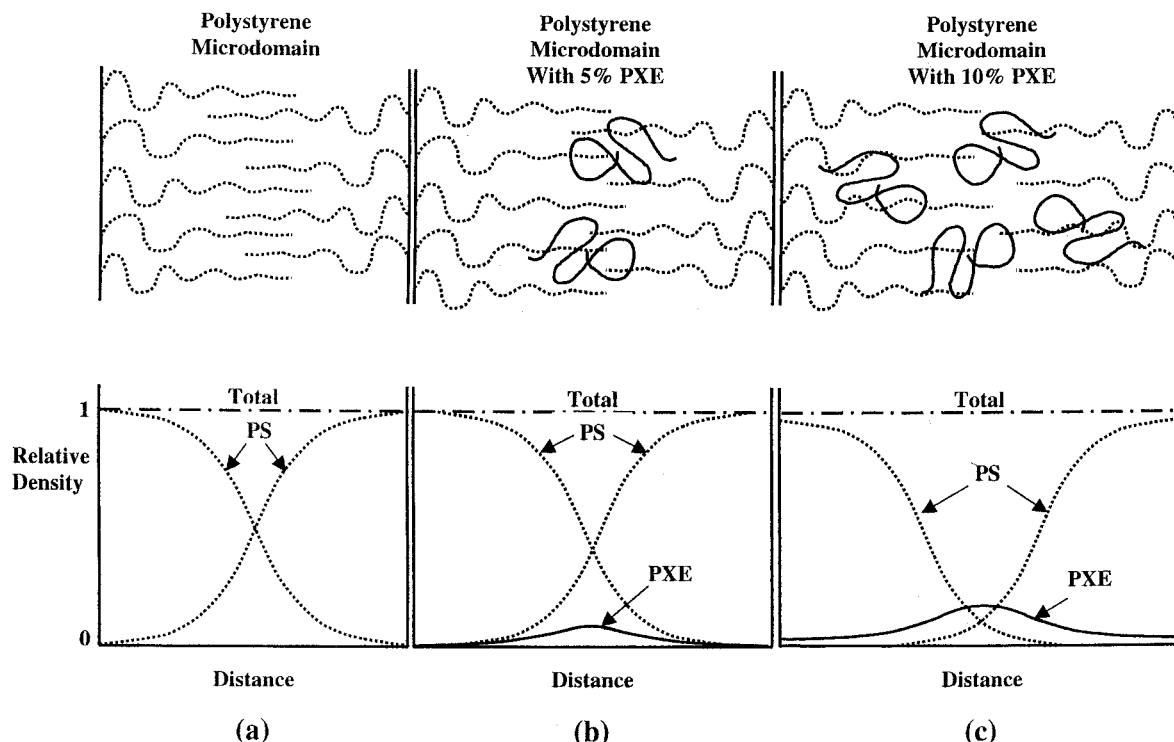


Figure 4. Schematic representation of the distribution of PXE homopolymers solubilized within the PS microdomain of an SEBS triblock copolymer: (a) neat SEBS-1, (b) a blend of 5% PXE-2 in SEBS-1, (c) a blend of 10% PXE-2 in SEBS-1. In the top drawings, the PS end blocks and PXE homopolymers are represented as dotted and solid lines, respectively. In the bottom drawings, the dotted and solid curves represent the relative density or concentration of PS end blocks and PXE homopolymer, respectively.

Table 2. Transition Temperatures (°C) and Shear Storage Modulus for Blends of PXE-2 with SEBS-1

| wt % PXE-2 | secondary loss temp | primary loss temp | mixed microphase T_g predicted from (1) | macrophase loss temp | order-disorder transition temp | $\log G'$ at 60 °C and 0.1 Hz (Pa) | total wt % of glassy phase |
|------------|---------------------|-------------------|---|----------------------|--------------------------------|------------------------------------|----------------------------|
| 0 | | 74 | | | 142 | 5.34 | 31.8 |
| 5 | 70 | 90 | 84 | | 180 | 6.49 | 35.2 |
| 10 | 88 | 111 | 93 | | 201 | 6.92 | 38.6 |
| 20 | 116 | 137 | 107 | 158 | 221 | 7.00 | 45.4 |
| 30 | | 131 | 120 | 161 | 251 | 7.03 | 52.3 |
| 40 | | 131 | 134 | | | 7.16 | 59.1 |

has an unfavorable interaction with the EB block of the copolymer. If PXE is depleted at the microdomain interface but is totally solubilized within the polystyrene microdomain, the concentration at the center of the polystyrene microdomains must necessarily be enriched in PXE. The secondary loss process for the 5% blend, for example, begins at a temperature comparable to the T_g of the polystyrene block of neat SEBS, indicating that the depleted regions within the polystyrene microdomains contain almost no PXE homopolymer. The primary loss temperature occurs at 90 °C, suggesting that the composition near the center of the microdomain reaches nearly 10% PXE, about twice the global concentration. The proposed nature of the PXE gradients is represented schematically in Figure 4. While the determination of a primary and secondary loss transition temperature is somewhat artificial because of the broad nature of the loss transitions, the two transition temperatures reported do correctly reflect the overall trends in loss transition behavior. Both loss transition processes increase in temperature as more PXE homopolymer is added, indicating that the PXE concentration increases in both the depletion and excess regions of the PXE concentration gradients as depicted in Figure 4.

The shapes of the $\tan \delta$ curves undergo a fundamental change for blend compositions exceeding 10%. The loss transitions become significantly broader, and a new

shoulder develops at a temperature near 160 °C, the glass transition of neat PXE-2. The loss transitions for these compositions span the entire temperature range between the glass transitions of neat PXE-2 and the styrene block in neat SEBS-1. Some of the PXE-2 exists in a pure state for these compositions, suggesting that saturation of the PS microdomain and the onset of a PXE-2 macrophase separation transition occurs at a composition between 10% and 20% PXE-2.

Application of the Fox equation to the two apparent T_g 's of the 30% blend shows that PXE-2 resides within a range of environments: an essentially pure PXE-2 macrophase and within a gradient of concentration in a PXE-saturated PS microphase containing about 77 wt % on average of PXE-2. Because the PXE-2 is heterogeneously distributed within the saturated microphase, it is not possible to stipulate an exact composition for the saturated polystyrene microphase.

Loss data for the 40% blend (not shown) can only be recorded up to a temperature of about 110 °C, above which the sample loses integrity. The loss data up to 110 °C superimpose over that of the 30% blend. The loss processes associated with the polystyrene microdomains are therefore identical for the 30% and 40% blends, as they should be if the PXE saturation concentration of the polystyrene microdomains is exceeded and PXE macrophases are present. Experimental loss transition

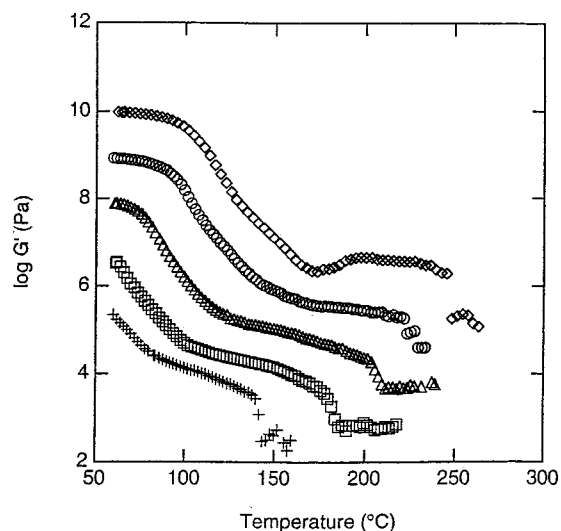


Figure 5. Shear storage modulus as a function of temperature for blends of PXE-2 with SEBS-1. From bottom to top, the compositions are 0, 5, 10, 20, and 30 wt % PXE-2. The 10, 20, and 30 wt % blend modulus values have been multiplied by 10, 100, and 1000, respectively, to improve clarity.

temperatures are summarized in Table 2. The change in macroscopic mechanical behavior at 40% PXE is the result of a morphological transition to a continuous glassy phase as the total glass concentration (mixed PXE and polystyrene) becomes about 60%. Catastrophic softening for the 40% blend therefore occurs at the lowest T_g of the continuous glassy phase and not at the T_{odt} as observed for lower composition blends with a continuous rubbery phase.

The temperature dependence of the shear storage modulus for blends of PXE-2 with SEBS-1 is shown in Figure 5. The T_{odt} is manifest as a drop of about 1 order of magnitude in the shear storage modulus above the rubbery plateau region. A clear trend of increasing T_{odt} is seen in Table 2 for the 5–30 wt % blends. The phase behavior of the blends is also reflected in the magnitude of the shear storage modulus. For the 0 and 5% blends, no indication of a glassy plateau is seen. The 10% blend shows a small glassy plateau from 60 to 80 °C. The plateau is extended to wider temperature ranges for the 20% and 30% blends as more glass is added into the PS microphase, and the blend T_g increases.

An estimate of the saturation concentration, or the onset of macrophase separation, can be obtained by examining the shear storage modulus in the glassy plateau region as a function of the PXE-2 concentration. The shear storage modulus at 60 °C was chosen for comparison sake and will be referred to as the plateau modulus. The plateau modulus (Table 2) levels off at about 20% PXE. Below 20%, the added PXE-2 is associating with the PS microphase, causing an increase in the T_g and plateau modulus. Above 20%, the plateau modulus does not appreciably change with PXE-2 content, and a second primary loss transition appears near the T_g of neat PXE, indicating the formation of essentially pure PXE macrophases.

PXE-2 addition also causes significant changes in the rubbery plateau region of the shear storage modulus curves for the blends (see Figure 5). The 5% blend shows an elevation in the shear modulus over the entire temperature range compared to neat SEBS-1. The modulus in the rubbery plateau region falls off slowly

Table 3. Optical Clarity

| material | concn of added PXE homopolymer | | | | | |
|--------------|--------------------------------|--------|-------|-------|-------|--------|
| | 0 | 5 | 10 | 20 | 30 | 40 |
| neat SEBS-1 | clear | | | | | |
| PXE-1/SEBS-1 | | clear | clear | | | |
| PXE-2/SEBS-1 | | clear | clear | clear | clear | cloudy |
| PXE-6/SEBS-1 | | cloudy | | | | |

in all of the materials until there is a drastic drop associated with the T_{odt} . The onset temperature and slope of the rubbery plateau increase with PXE content, the former effect resulting from the associated increase of the T_g of the polystyrene microphase. The terminal zone of the rubbery plateau region extends with PXE content due to the associated increase in the T_{odt} . It is also apparent that the breadth of the glass transition increases markedly with PXE content, consistent with the aforementioned inhomogeneous distribution of PXE within the microdomains. The somewhat unusual rubbery plateau behavior observed for the 30% blend may be associated with the presence of PXE-2 macrophases or to the formation of a bicontinuous morphology since the total glassy content is nearly 50%. The 40% blend does not show good mechanical integrity, most likely due to a phase inversion to a structure with a continuous glassy phase.

In summary, dynamic mechanical analyses demonstrate that the addition of PXE-2 to an SEBS triblock copolymer extends the upper use temperature of the material by increasing the mixed microphase glass transition temperature and increases the shear modulus. The improvement in mechanical properties comes at the cost of more difficult processing because the order–disorder transition temperature is elevated by blending and the viscosity of block copolymer systems remains high below the T_{odt} .

3. Blends of PXE with SEBS-1: Molecular Weight Effects. The solubility of PS homopolymers within the microdomains of styrenic block copolymers has been shown to depend strongly on the molecular weight of the added homopolymer. The homopolymer must normally have a molecular weight less than or equal to that of the associating block,^{15–17} to be soluble within the microdomain because of the limited conformations available to it in this confined geometry. It is unfavorable for a relatively large homopolymer to be solubilized within a microdomain, because it loses much of its configurational entropy and gains only a small amount of translational entropy upon mixing.¹⁸ The solubility of PXE in SEBS is expected to be higher than for PS because of the exothermic heat of mixing that can partially compensate for the unfavorable entropic effects associated with homopolymer confinement.

Macrophase separation can be crudely detected by assessing the optical clarity of the block copolymer blend films. If a material is only microphase separated, the film will be clear, while the film will appear cloudy if macrophase separation exists. Although film clarity can be used to indicate the presence of phase separated polymer, it cannot be used to determine that phase separation has not occurred because it is not sensitive to low amounts of macrophase separation. Table 3 summarizes the results of optical clarity observations.

The 5% blend of PXE-6 with SEBS-1 is cloudy, indicating some macrophase-separated polymer is present even at this low homopolymer content. The 30% blend with PXE-2 is interesting, because it is clear at room

Table 4. Transition Temperatures (°C) and Shear Storage Modulus for Blends of 5% PXE with SEBS-1

| designation | PXE T_g | PXE/PS MW ratio | secondary loss temp | primary loss temp | mixed microphase T_g predicted from (1) | order-disorder transition temp | log G' at 60 °C and 0.1 Hz (Pa) | total wt % of glassy phase |
|--------------|--------------|--------------------|------------------------|----------------------|---|-----------------------------------|--------------------------------------|-------------------------------|
| neat SEBS-1 | | | | 74 | | 142 | 5.34 | 31.8 |
| PXE-1/SEBS-1 | 116 | 0.30 | 74 | 95 | 79 | 176 | 6.43 | 35.2 |
| PXE-2/SEBS-1 | 161 | 0.55 | 70 | 90 | 84 | 180 | 6.45 | 35.2 |
| PXE-6/SEBS-1 | 196 | 1.69 | 68 | 86 | 87 | 160 | 6.55 | 35.2 |

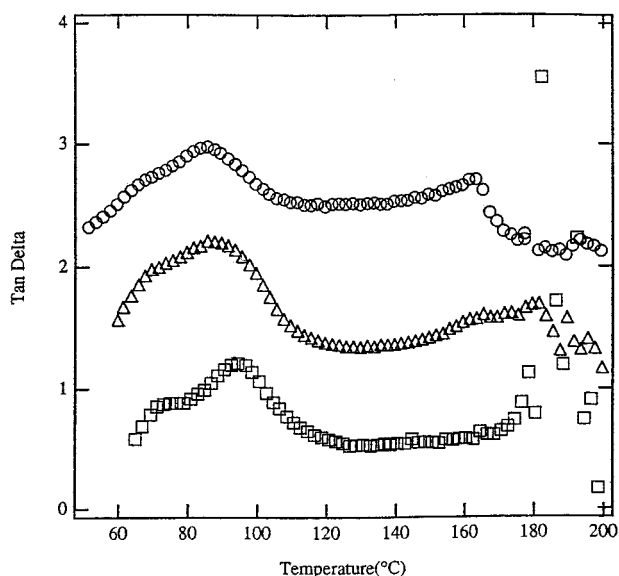


Figure 6. Tan δ as a function of temperature for 5 wt % blends of PXE with SEBS-1: PXE-1 blend (open squares), PXE-2 blend (open triangles), and PXE-6 blend (open circles). The PXE-2 data have been vertically offset by a factor of 1 and the PXE-6 data by a factor of 2 to improve clarity.

temperature, but clouds upon heating, consistent with the expected behavior for PS and PXE homopolymers. The 40% PXE-2 blend is unique in that it exhibits signs of stress cracking upon deformation, an indication that the glassy phase is continuous at this composition.

The loss tangent temperature dependence for 5% blends of PXE-1, PXE-2, and PXE-6 with SEBS-1 is shown in Figure 6. Primary and secondary loss transitions were observed for all blends, and their temperatures are summarized in Table 4. The loss transition temperatures for the blends decrease slightly with increase in molecular weight, even though the T_g 's of PXE homopolymers (Table 1) and the predicted T_g 's for completely mixed microphases calculated from (1) increase with PXE molecular weight. The most obvious explanation for this unanticipated decrease is that miscibility generally decreases with molecular weight. That is, the solubility of PXE within the block copolymer microdomains should decrease as its molecular weight increases. Optical clarity observations and electron microscopy measurements,⁸ however, detect macrophase separation only in the 5% PXE-6 blend. The results reported in the preceding section showed that the onset of macrophase formation occurs at a concentration of about 10–20% for PXE-2 blends. All of the homopolymer therefore appears to be solubilized in the 5% PXE-2 blend, and a similar situation is expected for the 5% blend with the lower molecular weight PXE-1. The molecular weight ratio of homopolymer to end block (Table 4) also favors miscibility for PXE-1 and PXE-2 blends. The order-disorder transition temperatures (Table 4) for 5% blends with PXE-1 and PXE-2 are about

the same as would be expected if all of the PXE is solubilized. The T_{odt} for the 5% PXE-6 blend, on the other hand, is depressed because macrophase formation decreases the total amount of PXE solubilized within the block copolymer microdomains. Macrophase separation can therefore provide at best a partial explanation for the molecular weight dependence of the loss transitions on molecular weight and does so only for the 5% PXE-6 blend.

The observed changes in loss transitions for 5% blends with PXE-1 and PXE-2 are therefore most likely associated with changes in the spatial distribution of solubilized PXE. Although the errors in determining the reported transition temperatures for the mixed end block microphases are large, the observed differences in loss transition temperatures are outside the error of measurement, and the observed shift in the loss transitions to lower temperatures evident upon increase in PXE molecular weight from the PXE-1 to the PXE-2 blend is significant. The breadth and bimodal character of the loss peaks in Figure 6 also diminish somewhat from PXE-1 to PXE-2. Assuming that the broad nature of the loss transitions is due to the heterogeneous distribution of PXE within the polystyrene end block microdomain, these trends suggest that the spatial distribution of solubilized PXE homopolymer is more heterogeneous for lower molecular weight PXE. This trend is opposite to what has been observed¹³ and predicted¹² for blends of A-type homopolymers with AB diblock copolymers (i.e., A/AB blends), where lower molecular weight A-type homopolymer additives are more homogeneously distributed within the A-type microdomain. Additional experiments and theory are clearly required to thoroughly examine the interesting possibility that homopolymer localization increases with molecular weight for blends of PXE with SEBS-1.

PXE blends with SEBS-1 might be expected to behave differently than the previously studied A/AB blends because of the fundamental difference in the nature of their interactions. In A/AB blends, the lower molecular weight additives gain translational entropy by locating more randomly, and there is no net change in the enthalpy of mixing because the homopolymer and block copolymer sequence are of the same species. In the case of C/ABA blends, as are studied herein, the gain in translational entropy by a more homogeneous spatial distribution may be partially offset by the exothermic heat of mixing of the type C homopolymer (PXE) with the type A end block (PS). Furthermore, these enthalpic effects may be concentration dependent. The PXE homopolymer distribution is ultimately determined by a complex balance of effects, including the translational entropy of the homopolymer, the overall enthalpy of mixing, the configurational entropy of the block copolymer, and the configurational entropy of solubilized homopolymer. These preliminary results provide motivation for new theoretical studies that consider the nature of the heterogeneous homopolymer distribution

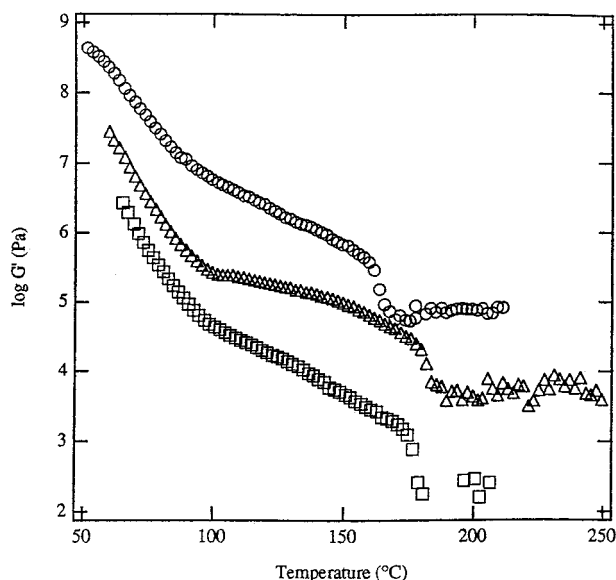


Figure 7. Shear storage modulus as a function of temperature for 5 wt % blends of PXE with SEBS-1: PXE-1 blend (open squares), PXE-2 blend (open triangles), and PXE-6 blend (open circles). The PXE-2 data have been multiplied by a factor of 10 and the PXE-6 data by a factor of 100 to improve clarity.

in C/ABA blends and how it depends on molecular weight.

The temperature dependence of the shear storage modulus for 5% blends of PXE-1, PXE-2, and PXE-3 with SEBS-1 is shown in Figure 7, and the T_{odt} 's are summarized in Table 4. The T_{odt} 's for the blends are all higher than that of the neat copolymer, because the favorable specific interactions between PXE and the PS end blocks stabilize the microphase structure. As a comparison, SEBS-1 blends containing 5% of fully solubilized polystyrene and polybromostyrene homopolymers with molecular weights similar to that of PXE-2 exhibit T_{odt} 's of 140 and 147 °C, respectively,⁸ much lower than the 180 °C transition seen for the 5% PXE-2 blend. PXE-1 has a similar stabilizing influence as PXE-2; however, the order-disorder transition temperature of the PXE-6 blend is significantly lower due to macrophase separation as alluded to earlier.

Values of the plateau modulus for the three PXE blends with SEBS-1 are summarized in Table 4. The weight percent of glassy phase refers to the combined weight percent of PXE and PS in the blend. All three PXE blends show a plateau shear modulus that is 1 order of magnitude greater than that of neat SEBS-1, indicating substantial reinforcement of the PS microdomains by PXE. The modulus increases only slightly with homopolymer molecular weight. The occurrence of macrophase separation in the PXE-6 blend does not compromise the enhancement in the shear modulus.

The dynamic mechanical analyses suggest that lower molecular weight PXE additives are most effective in modifying the properties of SEBS triblock copolymers because they provide the highest use temperatures (i.e., they yield the greatest elevation in the loss transition temperature for the end-block microdomain) and significant enhancement in the modulus, without requiring significantly higher processing temperatures (i.e., T_{odt}).

B. Flow Point Measurements and Cloud Point Curves. The measured flow temperatures (i.e., T_{odt} 's) for 0–40% blends of PXE-2 with SEBS-1 agree well with order-disorder transition temperatures determined by

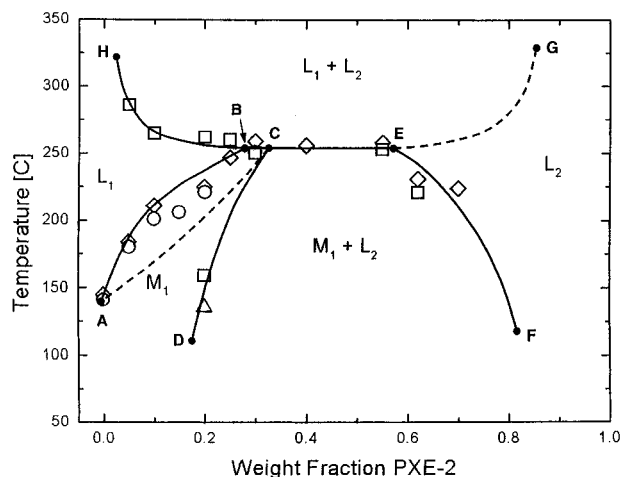


Figure 8. Phase diagram showing experimental thermal transitions and phase regions for blends of PXE-2 with SEBS-1. The measured transitions are rheological order-disorder (open circles), flow (open diamonds), light scattering cloud points (open squares), and the concentration at which a glass transition for pure PXE-2 is first observed (open triangle). The phase regions are M_1 (microphase-separated SEBS-1 containing PXE-2 solubilized within the PS microdomains), L_1 (disordered, homogeneous mixture of PXE-2 and SEBS-1, rich in SEBS-1), and L_2 (disordered, homogeneous mixture of PXE-2 and SEBS-1, rich in PXE-2). The dashed lines indicate phase transitions that were not observed experimentally, but that should theoretically be present.

dynamic mechanical analysis as shown in Figure 8. The flow method provides a more facile means for determining the T_{odt} compared to traditional methods such as scattering^{19,20} or rheological testing¹¹ and can be applied to blends containing more than 30% homopolymer that are not amenable to dynamic mechanical analysis. The flow technique does require a relaxation time on the order of seconds for the order-disorder process, however, and may not work for all block copolymers. For the low molecular weight SEBS-1, the PS molecular weight is well below the critical molecular weight for entanglement and the relaxation time is short. For higher molecular weight block copolymers, the relaxation time may be significantly longer, and the method may not give an accurate indication of T_{odt} .

Light scattering cloud points indicating changes in opacity upon heating are represented by the open squares in Figure 8. In most cases, clouding was observed upon heating, indicating LCST behavior. The 20% blend shows clearing upon heating from region ($M_1 + L_2$) to region M_1 and then clouds upon going from region L_1 to region ($L_1 + L_2$). The former clearing transition is in agreement with the onset of a PXE-2 macrophase T_g , indicated by the open triangle in Figure 8. Cloud points at point C and along curve EF are consistent with measured flow points (open diamonds).

C. Phase Diagrams. The availability of T_{odt} and T_g data, cloud point temperatures, flow temperatures, and saturation concentration data for the PXE-2 blends allows the partial phase diagram shown in Figure 8 to be constructed. The lower portion of the diagram below the phase envelope DCEF is a two-phase region, exhibiting upper critical solution temperature (UCST) behavior. Within this region, microphase-separated SEBS-1 containing PXE-2 solubilized within the PS microdomain (phase M_1) is in equilibrium with a homogeneous, disordered mixture of PXE-2 and SEBS-1 that is rich in PXE-2 (phase L_2). Similar low-temperature

UCST behavior was reported by Roe²¹ for a blend of poly(styrene-*b*-butadiene) with PS and was predicted by Whitmore and Noolandi²² for blends of AB diblock copolymers with type A homopolymers. The phase line CD was determined by noting the concentration at which the shear modulus levels off in Table 2 by measuring cloud points upon heating and by noting the concentration at which a loss transition associated with pure PXE-2 is first observed. The lines CE and EF were determined by measuring flow temperatures and cloud point temperatures upon heating.

An order-disorder transition coexistence region exists within the area ABCA in Figure 8, indicating equilibrium between phases M_1 and L_1 , where L_1 is a homogeneous, disordered mixture of PXE and SEBS-1 that is rich in SEBS-1. These transitions were measured by dynamic mechanical and flow point analyses. The Gibbs phase rule defines the number of phases present in the phase diagram and specifies that a single transition line cannot separate two single-phase regions if the transition is first order.²³ Leibler²⁴ determined the order-disorder transition to be first order in nature, necessitating the presence of a two-phase envelope at the T_{odt} . The envelope drawn has been exaggerated in size to emphasize its existence.

The upper portion of the phase diagram indicates lower critical solution temperature (LCST) behavior above the region defined by the phase envelope HBCEG. Within this region there is equilibrium between a SEBS-1-rich disordered macrophase (L_1) and a PXE-2-rich disordered macrophase (L_2). The macrophase separation that occurs upon heating is similar to that observed for blends of PS and PXE homopolymers. The line BCE indicates the peritectic temperature, where phases M_1 , L_1 , and L_2 coexist. Existence of the peritectic is confirmed by the flow temperature of the 40% PXE-2 blend.

The phase diagram presented in Figure 8 reflects the trends predicted by equation-of-state calculations²⁵ for blends of PS and PXE homopolymers of equal molecular weight. For molecular weights below 10 kg/mol, miscibility at all compositions and temperatures is predicted up to 400 °C. For blends of 10 kg/mol molecular weight homopolymers, both UCST and LCST behavior are predicted, indicating a miscibility window. As the molecular weight increases, the miscibility window becomes narrower and eventually closes altogether.

In the case of SEBS-1 blends with PXE-2, the LCST portion of the phase diagram is controlled by interactions between PXE and the PS block copolymer sequence and should exhibit similar behavior to blends of PXE and PS homopolymers. The UCST behavior predicted in calculations for PS and PXE homopolymer blends does not appear in the experimental phase diagram because it occurs below room temperature for the molecular weights of interest. Instead, the experimental low-temperature UCST phase behavior is associated with the repulsive interactions between PXE and the EB copolymer segment, as is the case for blends of polystyrene with styrenic block copolymers.

The effects of PXE molecular weight on the phase diagrams can be inferred from the anticipated effects of molecular weight on the phase behavior of the respective homopolymer blends. Increased PXE molecular weight additives should depress the LCST curve related to their attractive interactions with the PS sequence and elevate the UCST curve associated with their repulsive interactions with the EB sequence. Both

regions of coexistence ($L_1 + L_2$ and $M_1 + L_2$ in Figure 8) should subsequently broaden with increase in PXE molecular weight. The absence of macrophase formation in the 5% PXE-1 and 5% PXE-2 blends coupled with the observation of macrophases in the PXE-6 blend confirms the anticipated broadening of the UCST region ($M_1 + L_2$ in Figure 8) with increase in molecular weight. The width of the peritectic line (BCE in Figure 8) should also increase with increasing molecular weight, but it is not possible to predict the change in the peritectic temperature without a rigorous theory. It can be concluded, however, that an increase in PXE molecular weight will shrink the range of optimal processing conditions indicated by region L_1 in Figure 8.

From a practical point of view, the phase diagram contains useful information about processing windows and use temperatures for PXE-2/SEBS-1 blends as well as solubility limits of PXE-2 in the PS microdomain. Phase L_1 is the region of optimum processing conditions, because above the T_{odt} the physical cross-links of the system have been removed and the melt viscosity is sufficiently reduced to permit extrusion or molding. Processing within the coexistence regions ($L_1 + L_2$) or ($M_1 + L_2$) may be problematic and lead to heterogeneous properties upon cooling to room temperature due to the nonequilibrium nature of two-phase flow.

The optimal range of room temperature applicability for PXE-2 blends is within region M_1 , up to a concentration of about 20% PXE-2. Here the EB microphases are rubbery and continuous, while the glassy mixed microphase of PXE solubilized within the PS microphases provides excellent reinforcement of the continuous rubber matrix and significant enhancement of the mechanical properties. Blends that fall within region ($M_1 + L_2$) also show excellent property enhancement as long as the concentration of PXE-2 is below about 30% where the glassy phase becomes continuous. Processing may be problematic for blends in this region, however, because phase L_1 is not accessible, and processing within regions ($L_1 + L_2$) or ($M_1 + L_2$) may lead to nonequilibrium effects and poor quality control.

Lower molecular weight PXE homopolymers are the most effective additives because the L_1 phase for processing and the M_1 region of applicability extend to higher concentrations as molecular weight decreases. The higher solubility limit for lower molecular weight PXE allows higher modulus values and more elevated glass transition temperatures to be obtained.

Summary

The influence of the molecular weight and concentration of PXE end block associating homopolymers on the thermomechanical properties and phase behavior of a SEBS triblock copolymer are reported. These homopolymers exhibit high-temperature LCST behavior with the PS end block and low-temperature UCST behavior with the EB midblock of the copolymer. Experimental data are used to construct phase diagrams that show properties changes, identify end-use regions of composition, and indicate appropriate conditions for optimal processing. PXE homopolymer addition is shown to be an interesting and viable route to improve or modify the properties of SEBS triblock copolymers, since it generally causes elevation and extension of the rubbery plateau, enhancement of the room temperature shear modulus, an increase in the upper use temperature, and an increase in the order-disorder transition tempera-

ture. The results demonstrate that homopolymers in the oligomer range of molecular weight are most useful for this purpose because they are readily solubilized within the end-block microdomains.

Acknowledgment. The authors acknowledge financial support provided through grants from the Shell Development Company and the University of Connecticut Research Foundation and are grateful to Dr. B. Hsiao for assistance with some of the light scattering experiments.

References and Notes

- (1) Diamant, J.; Soong, D.; Williams, M. *Polym. Eng. Sci.* **1982**, 22, 673.
- (2) Tse, M. F. *J. Adhes. Sci. Technol.* **1989**, 3, 551.
- (3) Roe, R. J. *Polym. Eng. Sci.* **1985**, 25, 1103.
- (4) Han, C. D.; Baek, D. M.; Kim, J.; Kimishima, K.; Hashimoto, T. *Macromolecules* **1992**, 25, 3052.
- (5) Tucker, P. S.; Barlow, J. W.; Paul, D. R. *Macromolecules* **1988**, 21, 1678.
- (6) Tucker, P. S.; Barlow, J. W.; Paul, D. R. *Macromolecules* **1988**, 21, 2794.
- (7) Hashimoto, T.; Kimishima, K.; Hasegawa, H. *Macromolecules* **1991**, 24, 5704.
- (8) Baetzold, J. P. PhD Dissertation, University of Connecticut, 1990.
- (9) Koberstein, J. T.; Russell, T. P.; Walsh, D. J.; Pottick, L. *Macromolecules* **1990**, 23, 877.
- (10) Hay, A. S. *Polym. Sci. Eng.* **1976**, 16, 1.
- (11) Almdal, K.; Rosedale, J. H.; Bates, F. S. *Macromolecules* **1990**, 23, 4336.
- (12) Shull, K. R.; Mayes, A. M.; Russell, T. P. *Macromolecules* **1993**, 26, 3929.
- (13) Hashimoto, T.; Tanaka, H.; Hasegawa, H. *Macromolecules* **1990**, 23, 4378.
- (14) MacKnight, W. J.; Karasz, F. E.; Fried, J. R. In *Polymer Blends*; Paul, D. R., Newman, S., Eds.; Academic Press: New York, 1978; Vol. 1, p 185.
- (15) Aggarwal, S. L.; Livigni, R. A. *Polym. Eng. Sci.* **1977**, 17, 498.
- (16) Mayes, A. M.; Russell, T. P.; Satija, S. K.; Majkrzak, C. F. *Macromolecules* **1992**, 25, 6523.
- (17) Winey, K. I.; Thomas, E. L.; Fetters, L. J. *Macromolecules* **1991**, 24, 6182.
- (18) Hong, K. M.; Noolandi, J. *Macromolecules* **1983**, 16, 1083.
- (19) Zin, W. C.; Roe, R. J. *Macromolecules* **1984**, 17, 183.
- (20) Koberstein, J. T.; Russell, T. P.; Walsh, D. J.; Pottick, L. *Macromolecules* **1990**, 23, 877.
- (21) Roe, R.-J. *Polym. Eng. Sci.* **1985**, 25, 1103.
- (22) Whitmore, M. D.; Noolandi, J. *Macromolecules* **1985**, 18, 2486.
- (23) Gordon, P. *Principles of Phase Diagrams in Material Systems*; McGraw-Hill: New York, 1968.
- (24) Leibler, L. *Macromolecules* **1980**, 13, 1602.
- (25) Flory, P. J.; Orwoll, R. A.; Vrij, A. *J. Am. Chem. Soc.* **1964**, 86, 3567.

MA000933F